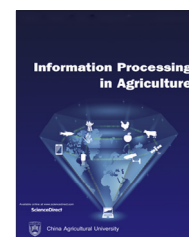


Available at www.sciencedirect.com

INFORMATION PROCESSING IN AGRICULTURE xxx (xxxx) xxx

journal homepage: www.elsevier.com/locate/inpa

Recognition and classification of paddy leaf diseases using Optimized Deep Neural network with Jaya algorithm

S. Ramesh*, D. Vydeki

Electronics and Communication Engineering Department, VIT University, Chennai 600127, India

ARTICLE INFO

Article history:

Received 25 March 2019

Received in revised form

28 August 2019

Accepted 6 September 2019

Available online xxxx

Keywords:

Paddy leaf diseases

Optimized Deep Neural Network

Jaya optimization algorithm

K-means clustering

Color features

Texture features

ABSTRACT

In the agriculture field, one of the recent research topics is recognition and classification of diseases from the leaf images of a plant. The recognition of agricultural plant diseases by utilizing the image processing techniques will minimize the reliance on the farmers to protect the agricultural products. In this paper, Recognition and Classification of Paddy Leaf Diseases using Optimized Deep Neural Network with Jaya Algorithm is proposed. For the image acquisition the images of rice plant leaves are directly captured from the farm field for normal, bacterial blight, brown spot, sheath rot and blast diseases. In pre-processing, for the background removal the RGB images are converted into HSV images and based on the hue and saturation parts binary images are extracted to split the diseased and non-diseased part. For the segmentation of diseased portion, normal portion and background a clustering method is used. Classification of diseases is carried out by using Optimized Deep Neural Network with Jaya Optimization Algorithm (DNN_JOA). In order to precise the stability of this approach a feedback loop is generated in the post processing step. The experimental results are evaluated and compared with ANN, DAE and DNN. The proposed method achieved high accuracy of 98.9% for the blast affected, 95.78% for the bacterial blight, 92% for the sheath rot, 94% for the brown spot and 90.57% for the normal leaf image.

© 2019 China Agricultural University. Production and hosting by Elsevier B.V. on behalf of KeAi. This is an open access article under the CC BY-NC-ND license (<http://creativecommons.org/licenses/by-nc-nd/4.0/>).

1. Introduction

In many countries, for human beings one of the important sources of earning is agriculture [1]. Based on the environmental conditions of land and need various food plants are harvested by the farmers. However, the farmers are facing

several problems like natural disasters, shortage of water, plant diseases, etc., [2]. By providing some technical facilities most of the problems are reduced. Carrying out the on time prevention from the disease may enhance the productivity of food and hence the search for the experts are not necessary [3]. In the agriculture domain one of the necessary research topics is the recognition of plant disease [4]. Recently, recognition and classification of plant diseases is a demanding task.

To avoid the losses in the quantity of agriculture products and in the yield, an important key is the recognition of plant diseases [5]. For the sustainable agriculture, disease recogni-

* Corresponding author.

E-mail addresses: s.ramesh2015@vit.ac.in (S. Ramesh), vydeki.d@vit.ac.in (D. Vydeki).

Peer review under responsibility of China Agricultural University.

<https://doi.org/10.1016/j.inpa.2019.09.002>

2214-3173 © 2019 China Agricultural University. Production and hosting by Elsevier B.V. on behalf of KeAi.

This is an open access article under the CC BY-NC-ND license (<http://creativecommons.org/licenses/by-nc-nd/4.0/>).

tion and health monitoring on plants is very harmful. The related studies of the recognition of plant diseases mean that the diseases are the visible patterns observed on the plants [6]. Manually, the plant diseases are more difficult for the monitoring process. For the manual process it needs more processing time, large amount of work and expertise in the diseases of plant. So that for the plant disease recognition, image processing techniques are utilized [7].

The image processing steps for the recognition of diseases comprise acquisition of images, pre-processing of images, segmenting the images, extracting the features and finally classification [8]. These techniques can be performed only on the external appearances of the infected plants [9]. Commonly, in most of the plants to detect the plant diseases, leaves are the important source. In rice plants, sheath rot, leaf blast, leaf smut, brown spot and bacterial blight are the most common diseases [10]. However for different plants, the symptoms of the plant diseases are varied. The plant diseases are different in color, size and shape and every disease has individual features. Some diseases have yellow color and some have brown color [11]. Some diseases are same in their shapes but differ in colors whereas, some are same in color but differ in their shapes. After the segmentation of diseased and normal portion the features related to disease can be extracted [12].

Normally, the manual detection of plant diseases is naked eye observation of experts which consumes more time, expensive on large farms [13]. It is difficult to process and also sometimes it produces an error when identifying the disease type [14]. Because of the unawareness of suitable management to rectify rice plant leaf diseases, the rice production is being reduced in recent years [15]. To overcome this a suitable and fast recognition system on rice leaf disease is needed. Hence this paper proposes a novel method for recognizing the diseases of rice plants using their images. This research mainly focuses on four most common rice plant diseases named as Brown spot, Leaf blast, Bacterial blight and Sheath rot. Our contribution in this work includes as follows: From the farm field in real world circumstances we captured the rice plant leaves images and prepared the dataset. Background elimination is carried out by the pre-processing. Segmentation is performed for clustering the diseased portion and the normal portion of the leaves. For the classification, optimized Deep Neural Network with Jaya algorithm is proposed. JOA is used for the best weight selection of DNN.

Rest of the paper is organized as follows: Section 2 contains the recent works related to rice plant disease classification. Section 3 defines the problem statement. Section 4 comprises our proposed methodology. Section 5 shows the experimental analysis. Section 6 represents the conclusion.

2. Related works

Some of the recent researches related to the recognition and classification of rice plant diseases are given as below.

On the basis of deep convolutional neural network, a novel rice plant disease detection approach was developed by Yang

Lu *et al.* [16]. They used a dataset which contains 500 images include diseased and non-diseased paddy stems and leaves. Classification was carried out with ten common rice diseases. They showed that their approach attained higher accuracy than the conventional machine learning method. The experimental outcomes represented the effectiveness and feasibility of their proposed model.

For the evaluation of ROI, a segmentation technique based on neutrosophic logic extended from the fuzzy set was introduced by Gittaly Dhingra *et al.* [17]. They used three membership functions for the segmentation. To detect the plant leaf as diseased or not feature subsets were considered on the basis of segmented regions. Various classifiers were employed for the demonstration and the random forest method overcome the other approaches. They used a dataset with 400 leaf images which included 200 diseased leaf image and 200 non-diseased leaf images.

Using image processing techniques, D. Nidhis *et al.* [18] developed a method for detecting the disease type affected by the paddy leaves. By evaluating the percentage of diseased area, the severity of the disease infection was calculated. Based on the severity of diseases the pesticides were utilized for the bacterial blight, brown spot and rice blast which are the main diseases affect the paddy crop and their productivity.

For the identification and the classification of rice plant diseases a new method was presented by Taohidul Islam *et al.* [19]. In their work, on the basis of percentage of RGB value of the diseased part, they detected and identified the diseases by employing image processing techniques. They utilized Naïve Bayes classifier which is a simple classifier to classify the disease into various classes. Their approach successfully recognized and classified three main types of rice plant diseases by using only one feature. Thus it was a faster method which required less time for computation.

Using the image processing techniques to automatically recognize the diseases in paddy leaves Gayathri Devi and Neelemegam [20] developed an approach. They used hybridized gray scale co-occurrence matrix, DWT and SIFT for the extraction of features. After extracting the features they were given to various classifiers include multiclass SVM, Naïve Bayesian, back propagation neural network and KNN for the classification of diseased and normal plants.

Aydin Kaya *et al.* [21] investigated the results of the effect of four different transfer learning models for deep neural network-based plant classification on four public datasets. Their experimental study demonstrated that transfer learning can provide important benefits for automated plant identification and can improve low-performance plant classification models.

Alessandro dos Santos Ferreira *et al.* [22] used the Convolutional Neural Networks to perform weed detection in soybean crop images and classified the weeds among grass and broadleaf. An image database was created containing over fifteen thousand images of the soil, soybean, broadleaf and grass weeds. The Convolutional Neural Networks used in this work represented a Deep Learning architecture that has achieved remarkable success in image recognition.

3. Problem definition

For detecting the leaf diseases, the conventional methods are human vision based approaches. In these cases seeking the expert advice is time consuming and very expensive. The human vision based methods suffer many drawbacks. The accuracy and precision of human vision approach is dependent on the eyesight of the person or expert hired. Machine learning based method enables to identify the types of diseases, make the right decision and to select proper treatment. One of the advantages of using machine learning based method is that it performs tasks more consistently than human experts. Therefore, to overcome the drawbacks of conventional methods there is a need for a new machine learning based classification approach. Very few recent developments were recorded in the field of plant leaf disease detection using machine learning approach and that too for the paddy leaf disease detection and classification is the rarest.

4. Proposed methodology

The proposed system is developed with five phases which include image acquisition, pre-processing, image segmentation, feature extraction and classification. The paddy leaf images are captured from the farm field and the dataset is created. The dimensions of the images are reduced and the background is removed in the pre-processing step. The next step is image segmentation in which k-means clustering method is applied to segment the normal portion and the diseased portion. Then the classification of diseases is performed by DNN_JOA method. After performing the classification, if the classification result is not satisfied a feedback is sent to the segmentation phase in order to precise the stability of the developed method. The process flow steps are shown in Fig. 1.

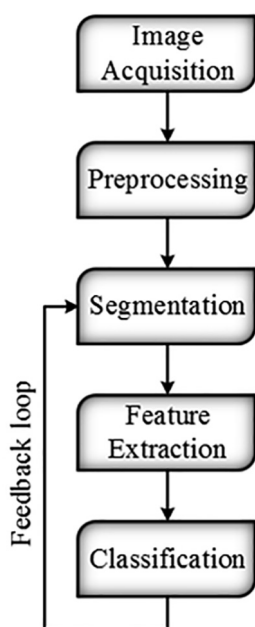


Fig 1 – Process flow steps.

4.1. Acquisition of images

Acquisition of images is the process of collecting the images which are used for this research. From the farm field in real world circumstances we captured the rice plant leaves images by using high resolution digital camera. Then for the recognition of diseases all the captured images are moved to the computer where the implementation process will be carried out. The dataset contains the images having the leaves with various degree of disease spread. The data set are collected from rural area of ayikudi and panpoli, Tirunelveli District, Tamilnadu. The images are captured and a dataset is prepared totally with 650 images which include 95 normal images, 125 bacterial blight images, 170 blast images, 110 sheath rot images and 150 brown spot images. Some of the sample images are given in (See Fig. 2).

4.2. Pre-processing

In pre-processing, for minimizing the requirement of memory and computation of power the images in the dataset are resized and cropped into the dimension of 300×450 pixels. In this phase an important thing is to eliminate the image background by applying hue values based fusion. Initially, the image in RGB model is converted into HSV. From the HSV model first the S value is considered for the process because it overs the whiteness. Based on the threshold value 90, the image is converted into a binary image and this binary image is fused with the original RGB image to create a mask. The threshold value is selected on the basis of several trials. The fusion process eliminates the background by assigning the pixel values as 0's. The pixel value 0 indicates black color in the RGB model. Only the leaf portion with the diseased part is present in this background removed image. Fig. 3 shows the preprocessing steps.

4.3. K-means clustering based segmentation

For the segmentation of image K-means clustering method is employed in this work. Clustering is a process to group the image into clusters. The diseased portion is extracted from the leaf image by this clustering. In a leaf image when applying this clustering the clusters are expected for the diseased part and the non-diseased part. This technique is applied on the hue part of the HSV model of the background removed image. Only the pure color is present in the hue component; it doesn't contain any information like brightness and darkness. On the basis of analysis of histogram of hue components centroid value is fed to generate perfect segments in order to overcome the randomness problem of the cluster. Moreover, from the diseased part cluster the unwanted green portion is eliminated.

From the background removed image for the hue component a histogram is created. Then, from the created histogram the hue values and the counts in every bin are extracted. On the basis of histogram and diseased image particular threshold value is found to differentiate the normal and the diseased portion. In two separate arrays, the hue values of both the normal portion and the diseased portion are stored. The histograms are shown in Fig. 4.

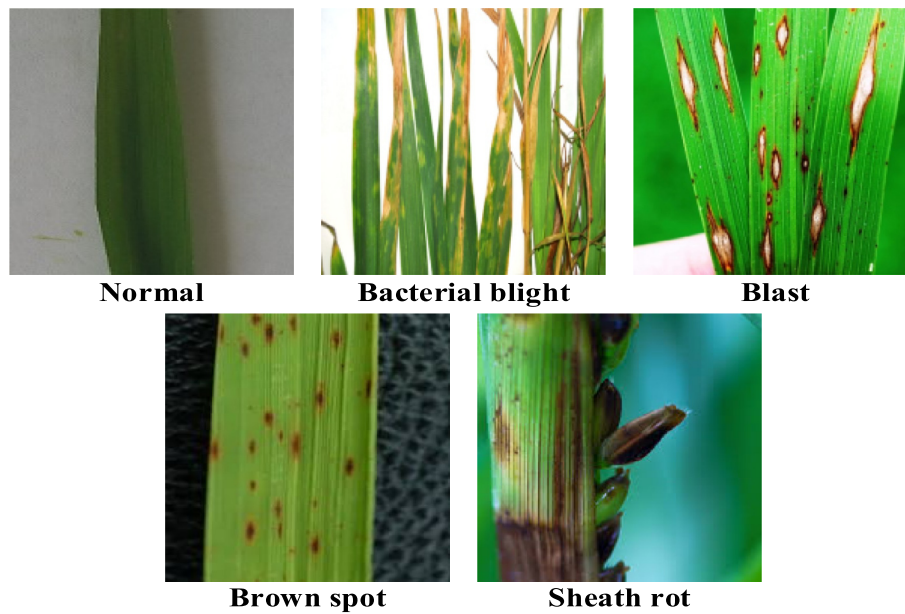


Fig 2 – Sample images of normal and diseased leaves.

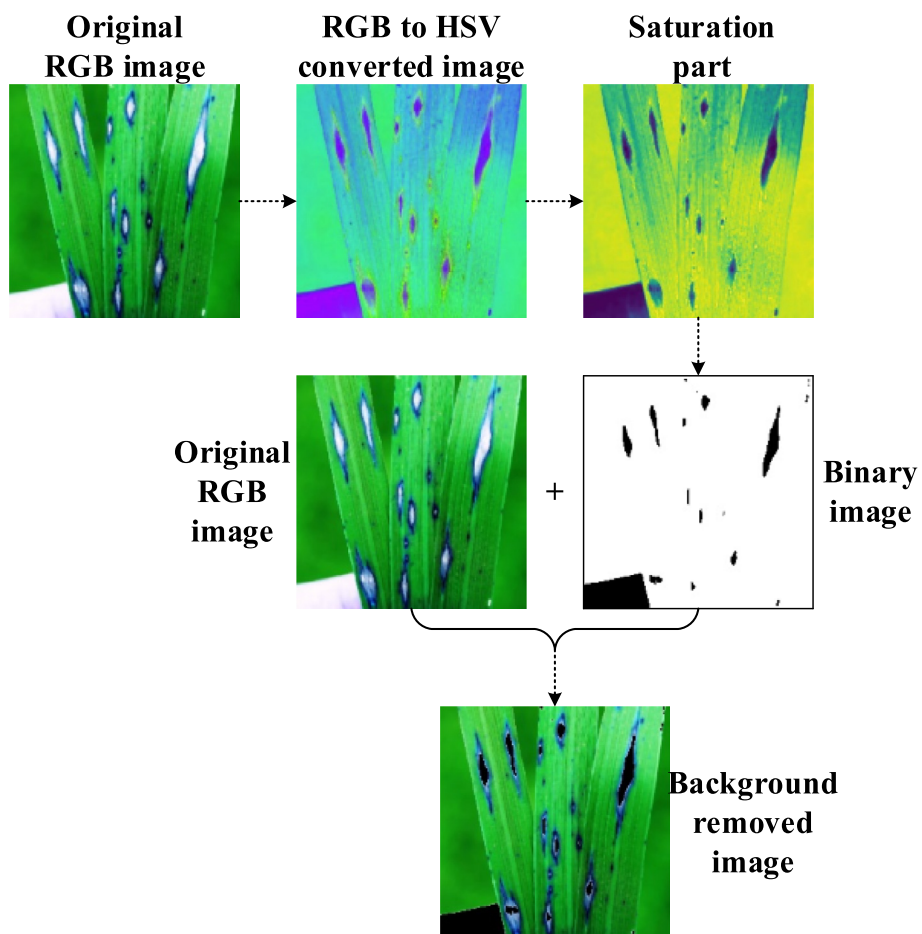


Fig 3 – Pre-processing steps for background elimination.

To select the centroid of each cluster, the highest value from the hue values of the normal and the diseased portion

are selected. The value of black color and the selected centroid values are fed in the clustering process. After clustering

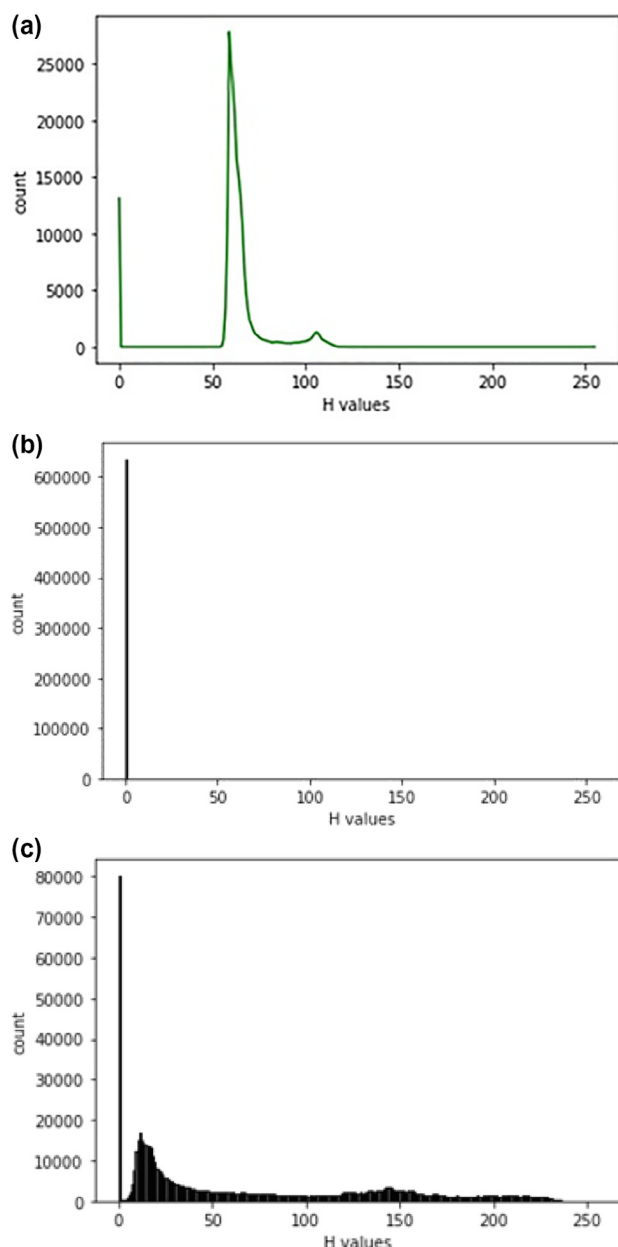


Fig 4 – (a) Histogram of hue part (b) Histogram of background removed blast affected portion (c) Histogram of background removed normal portion.

the image, the diseased portion contains unwanted green portion. In the calculation of features, the green pixels contributed adversely. So there may be a chance to affect the classification accuracy. In the hue model, the green color falls between 17.2 degree and 45 degree which are mapped as the minimum value of 0.048 and the maximum value of 0.125. Based on these maximum and minimum values, a binary mask is created for the removal of green color from the diseased portion.

Fig. 5 shows the clustered image from the hue part image. The output of the clustering is two clusters including normal portion and diseased portion.

4.4. Extracting features

In this work we extracted both the texture features and color features. The color features include extracting the mean values and standard deviation values whereas the texture features include the GLCM features such as homogeneity, contrast, correlation and energy.

4.4.1. Color features

- First the R, G and B components are extracted for the diseased portion and the mean value and the standard deviation are evaluated.
- From the HSV model, H, S and V components are extracted and the mean value is estimated.
- From the LAB color model, L, A and B components are extracted and the mean value is calculated.

The mean and standard deviation are calculated by using the formulas given below.

$$M_y = \frac{1}{n} \sum_{x=1}^n P_{yx} \quad (1)$$

$$S_y = \sqrt{\frac{1}{n} \sum_{x=1}^n (P_{yx} - M_y)^2} \quad (2)$$

where, n represents the total number of pixels, P_{yx} represents the pixel values.

4.4.2. Texture Features

Using the spatial relationship between the pairs of gray value intensity pixels, the GLCM captures the texture of the image. For the specified displacements homogeneity, correlation, energy and contrast are the features extracted from the GLCMs. The formulas for these features are given as below.

$$H_y = \sum_{x=0}^n \frac{P_{yx}}{1 + (y - x)^2} \quad (3)$$

$$Ct_y = \sum_{x=0}^n P_{yx}(y - x)^2 \quad (4)$$

$$Cn_y = \sum_{x=1}^n P_{yx} \frac{(y - M)(x - M)}{S_y} \quad (5)$$

$$E_y = \sum_{x=0}^n (P_{yx})^2 \quad (6)$$

where, H_y represents the homogeneity, Ct_y is the contrast, Cn_y denotes the correlation, E_y indicates the energy, n represents the total number of pixels, P_{yx} represents the pixel values, M_y represents the mean and S_y represents the standard deviation.

After extracting the color features and texture features, normalization is performed to normalize the feature values. For this normalization process Min-Max method is employed to normalize the values in the range of 0 to 1.

4.5. Optimized DNN based classification using JOA

The framework of DNN essentially contains three primary components which include input layer, output layer and

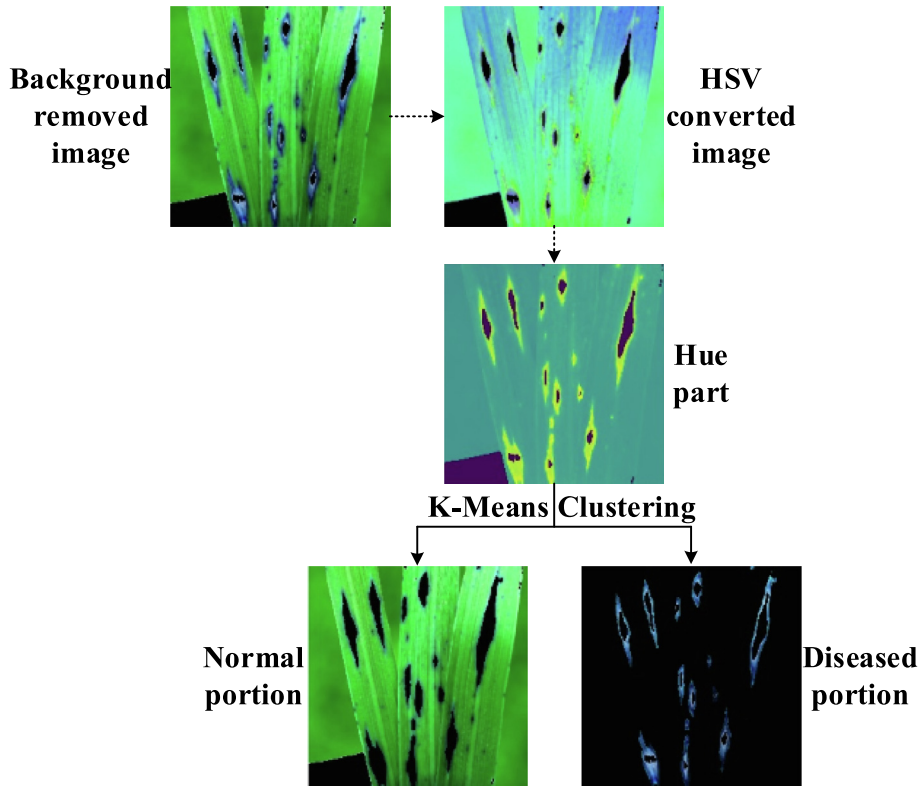


Fig 5 – Clustered image from the hue part.

hidden layers. The proposed architecture of DNN is shown in Fig. 6.

By considering the effort of preference weight fitness, the DNN is designed with two hidden layers for perfectly learning the mapping relation between the input and output data. In the training phase, by using the JOA the DNN iteratively

updates the weight of the nodes in the hidden layers. Due to the increase in the training iterations, this neural network continually fits the labelled training data's decision boundary. To enhance the training speed of the DNN and the classification accuracy, two hidden layers are constructed. In the hidden layer the total number of nodes is evaluated by using Eqn. (7).

$$n = \sqrt{a + b + c} \tag{7}$$

where, the number of input layer nodes is given as a , the number of output layer nodes is given as b , the number of hidden layer nodes is represented as n and a constant value between [1,10] is notated as c .

For enabling the non-linear fitness ability an activation function is added in the hidden layer of DNN. We have used the sigmoid as an activation function and it is given as,

$$S = \frac{1}{1 + e^{-x}} \tag{8}$$

The input data of the network is termed as x and it is activated by the mapping function M_f .

$$M_f = \text{sigm}(\omega_i x + \beta_i) \tag{9}$$

where, ω and β represents the weight matrix and the bias between the output layer and the hidden layer respectively.

To cause the representation space of the hidden neurons to align with human knowledge, we introduce another supervised loss function for DNN. In this case, we want to utilize the information contained in the data sample labels, which represent the human concepts. Given a conceptually labelled

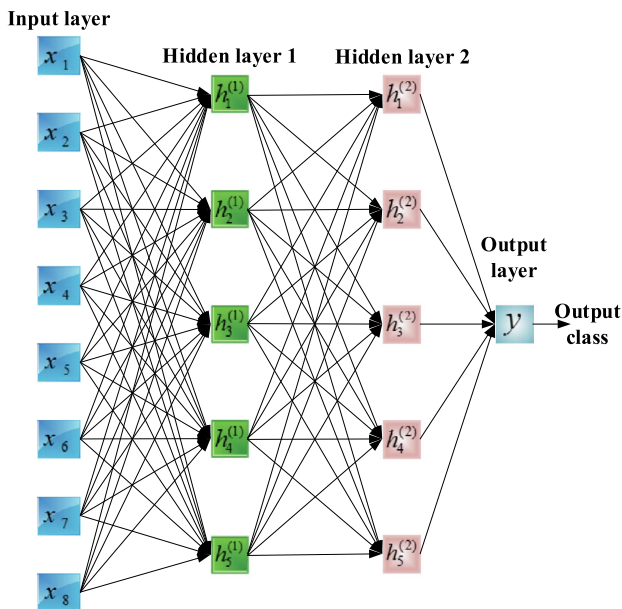


Fig 6 – Architecture of DNN with two hidden layers.

data sample (x, l) for a hidden layer, the loss form can be computed as

$$S(W_s, b_s; x, l) = \frac{1}{2m} \sum_{j=1}^m \|h_j(W_s, b_s; x) - l_j\|_2^2 \quad (10)$$

where W_s and b_s are the subsets of biases and m is the number of neurons in the hidden layer.

Cross entropy is used as the loss function of DNN as the preparation for training and testing. The use of cross-entropy losses greatly improved the performance of the sigmoid and softmax output models. The cross entropy loss is evaluated by the Eq. (11).

$$C_E = \frac{1}{n} \sum_{k=1}^n [Y_k \log \hat{Y}_k + (1 - Y_k) \log (1 - \hat{Y}_k)] \quad (11)$$

where, n represents the training sample quantity, Y_k indicates the k th actual output of training set, \hat{Y}_k is the k th expected output of testing set. We are using JOA algorithm for the optimal weight selection of DNN network.

In the population improving the fitness value of every solution is the main intention of JOA. By updating the values, this algorithm efforts the fitness value to shift towards the best solution. After that, the new solutions and the old solutions are compared and for the next iteration only the best solutions are considered. Moreover, it only requires tuning of the population size and number of iterations which leads to the implementation of the algorithm is simple as its solution is updated through only one phase using a single equation. It's dominant over other optimization techniques with respect to low computational complexity and time and faster

convergence speed. The implementation of this algorithm can be briefly summarized as follows:

Initialize the population size, the number of iterations and the termination criteria. From the population, the best and worst solutions should be determined with respect to the objective function. The current solution based on the best and worst solutions should be adjusted by using Eq. (12).

$$x'_{j,i,G} = x_{j,i,G} \times r_{1,j,G}^{(x_{j,best,G} - |x_{j,i,G}|)} - r_{2,j,G} \times (x_{j,worst,G} - |x_{j,i,G}|) \quad (12)$$

where $x_{j,best,G}$ and $x_{j,worst,G}$ are the values of the j th variable for the best candidate and the worst candidate, respectively; $r_{1,j,G}$ and $r_{2,j,G}$ are the random numbers in the range $[0, 1]$. The adjusted solution is compared with the previous solution. If the previous one is improved it will replace the previous solution else it will retain the previous solution [23]. The process is repeated from until the termination criteria are achieved. The flow chart for the best weight selection process is shown in Fig. 7.

4.6. Post-Processing

After performing the classification process, in order to precise the stability of the proposed method a feedback loop is generated in which the feedback is sent to the segmentation phase. In the segmentation phase a post-processing method, morphological opening is applied on the diseased segment to remove the green portion if there any exists. So that the performance of classification will be improved.

5. Experimental results

We implemented our proposed methodology using DNN JOA in Python platform version 3.6. The performance of our proposed method DNN-JOA is estimated and compared with the performance of existing classifiers such as ANN, DAE and DNN. The results are compared based on the disease classes which includes normal, bacterial blight, brown spot, sheath rot and blast disease. From the dataset 70% of images are used for training, 20% are used for testing and remaining 10% are used for validation.

Table 1 shows the classification performance of the DNN JOA method. Using the DNN JOA classifier the highest accuracy is achieved for the blast affected leaf image which is 98.9%.

Fig. 8 shows the confusion matrix obtained for our proposed method. From this confusion matrix the True Positive (TP), True Negative (TN), False Positive (FP) and False Negative (FN) values are predicted. The values of TP, TN, FP and FN from the above confusion matrix are 19, 109, 1 and 1 respectively for the normal image; the values of TP, TN, FP and FN are 22, 103, 2 and 3 respectively for the sheath rot; the values of TP, TN, FP and FN are 25, 102, 1 and 2 respectively for the brown spot; the values of TP, TN, FP and FN are 26, 99, 3 and 2 respectively for the bacterial blight; the values of TP, TN, FP and FN are 29, 98, 2 and 1 respectively for the blast affected image.

The graphs are shown for the performance metrics such as accuracy, F1-score, False Positive Rate (FPR), False Negative Rate (FNR), False Discovery Rate (FDR), Negative Predictive

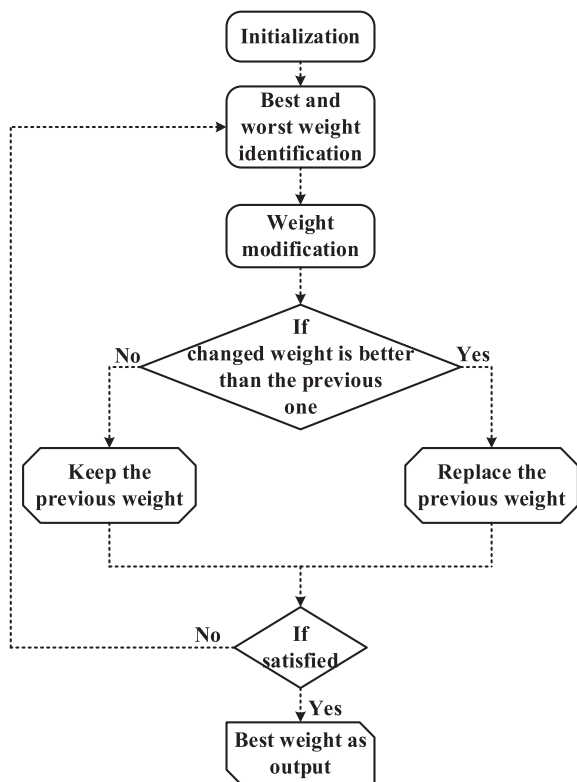


Fig 7 – Flow chart for the best weight selection using JOA.

Table 1 – Classification performance of diseased and normal leaf images.

Leaf type	Normal	Bacterial blight	Blast	Brown spot	Sheath rot
Accuracy	90.57	95.78	98.9	94	92
F1-score	81.25	88.75	96.86	85	91.86
Precision	73	80.4	92.8	85	75
FDR	17.1	19.5	10	26.6	25
FPR	6.2	4.7	1.8	4.4	5
FNR	10	14	5.7	7	8
TPR	75.6	89.5	92.6	85.5	75.3
TNR	90.7	91	98.1	94.5	95.9
NPV	91.2	95	97.4	93.6	96.1

Value (NPV), precision, True Positive Rate (TPR), True Negative Rate (TNR) and loss function.

Fig. 9 represents the comparison graph of accuracy for the five classes with respect to the four classifiers which includes the proposed and existing classifiers. When using our proposed method DNN_JOA the accuracy of normal image is

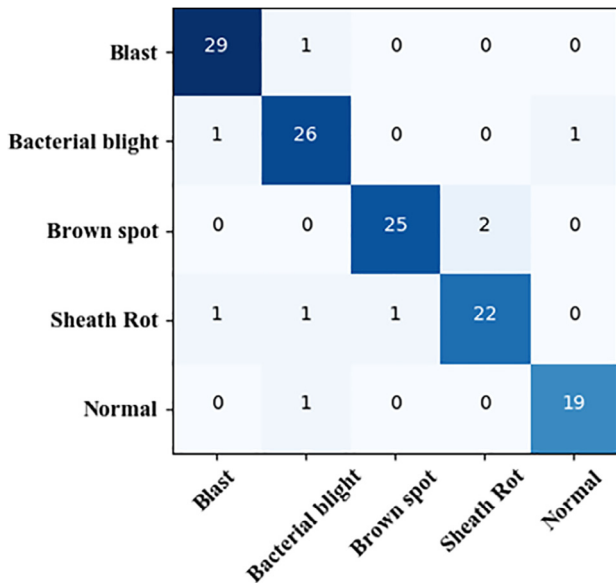


Fig 8 – Confusion Matrix of DNN-JOA.

90.57%, bacterial blight is 95.78%, blast is 98.9%, brown spot is 94% and sheath rot is 92%. When using ANN classifier the accuracy of normal image is 77.24%, bacterial blight is 78%, blast is 85%, brown spot is 81.5% and sheath rot is 78.3%. When using DAE classifier the accuracy of normal image is 81.4%, bacterial blight is 86.2%, blast is 91.5%, brown spot is 87.7% and sheath rot is 83.4%. When using DNN classifier the accuracy of normal image is 83%, bacterial blight is 91.7%, blast is 96.2%, brown spot is 90.6% and sheath rot is 88.5%.

Fig. 10 represents the comparison graph of F1-score for the five classes with respect to the four classifiers which includes the proposed and existing classifiers. When using our proposed method DNN_JOA the F1-score of normal image is 81.25%, bacterial blight is 88.75%, blast is 96.86%, brown spot is 85% and sheath rot is 91.86%. When using ANN classifier the F1-score of normal image is 61.45%, bacterial blight is 68.67%, blast is 74.89%, brown spot is 65% and sheath rot is 71.56%. When using DAE classifier the F1-score of normal image is 69.23%, bacterial blight is 74.68%, blast is 84.79%, brown spot is 76.45% and sheath rot is 79.98%. When using DNN classifier the F1-score of normal image is 72.68%, bacterial blight is 81%, blast is 88.58%, brown spot is 80.6% and sheath rot is 84.67%.

Fig. 11 represents the comparison graph of FPR for the five classes with respect to the four classifiers which includes the proposed and existing classifiers. When using our proposed

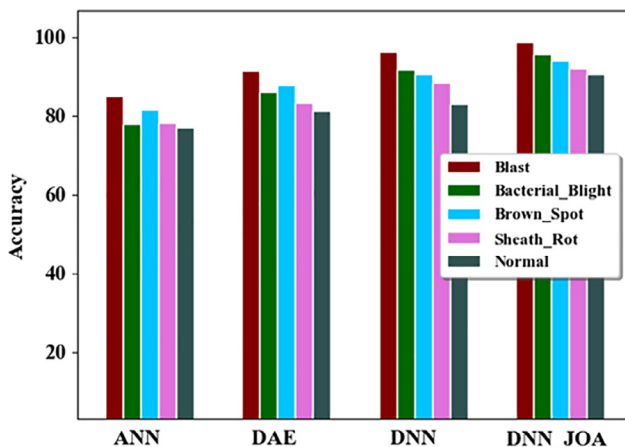


Fig 9 – Comparison graph of accuracy.

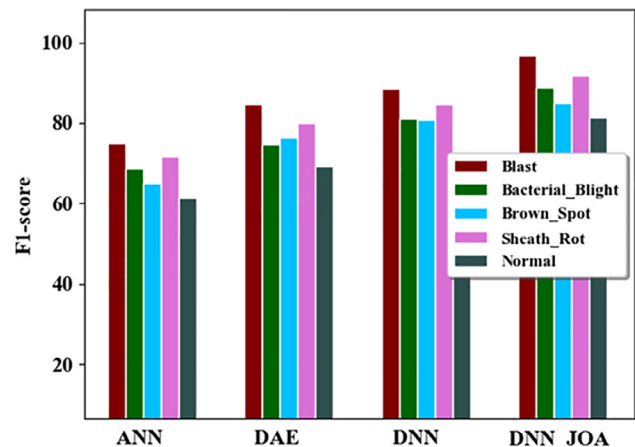


Fig 10 – Comparison graph of F1-score.

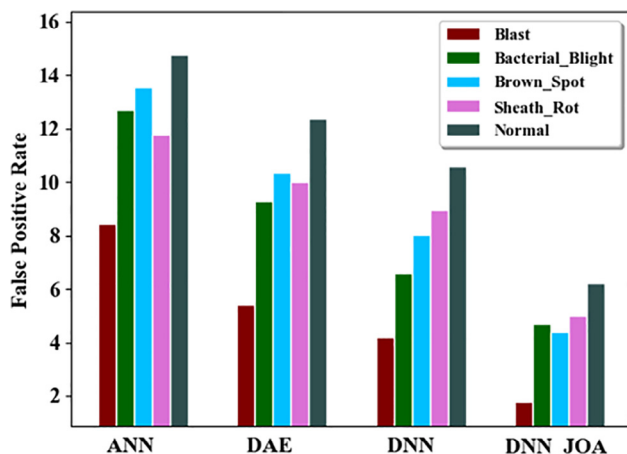


Fig 11 – Comparison graph of FPR.

method DNN_JOA the value of FPR of normal image is 6.2, bacterial blight is 4.7, blast is 1.8, brown spot is 4.4 and sheath rot is 5. When using ANN classifier the FPR of normal image is 14.78, bacterial blight is 12.7, blast is 8.45, brown spot is 13.56 and sheath rot is 11.78. When using DAE classifier the value of FPR of normal image is 12.3, bacterial blight is 9.3, blast is 5.4, brown spot is 10.3 and sheath rot is 9.9. When using DNN classifier the FPR of normal image is 10.6, bacterial blight is 6.6, blast is 4.2, brown spot is 8 and sheath rot is 8.9.

Fig. 12 represents the comparison graph of FNR for the five classes with respect to the four classifiers which includes the proposed and existing classifiers. When using our proposed method DNN_JOA the value of FNR of normal image is 10, bacterial blight is 14, blast is 5.78, brown spot is 8 and sheath rot is 7. When using ANN classifier the FNR of normal image is 22.6, bacterial blight is 23, blast is 14, brown spot is 22.5 and sheath rot is 20.1. When using DAE classifier the value of FNR of normal image is 19, bacterial blight is 21, blast is 10.4, brown spot is 17.8 and sheath rot is 18.3. When using DNN classifier the FNR of normal image is 17.8, bacterial blight is 17, blast is 9.18, brown spot is 14.5 and sheath rot is 14.6.

Fig. 13 represents the comparison graph of FDR for the five classes with respect to the four classifiers which includes the

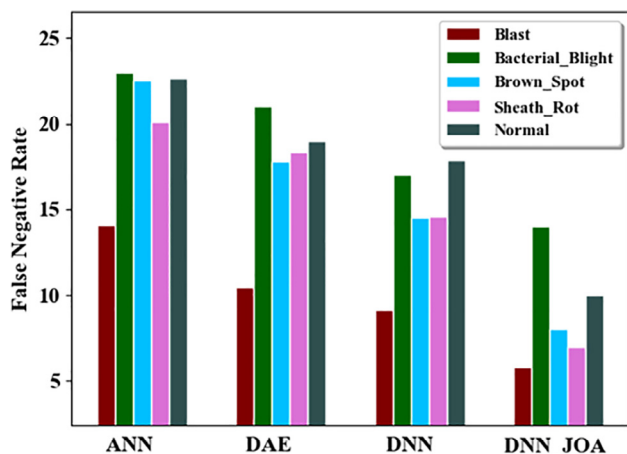


Fig 12 – Comparison graph of FNR.

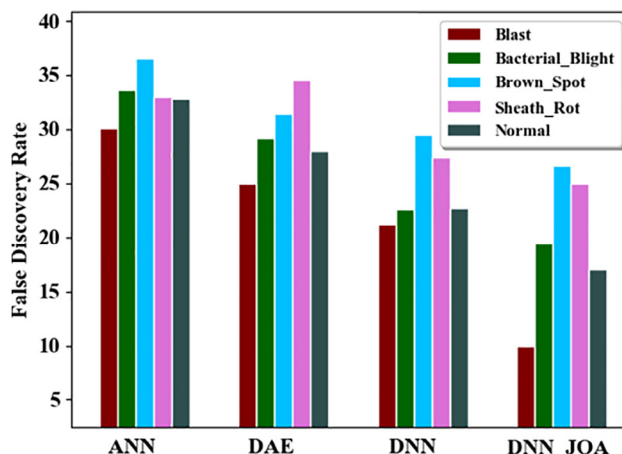


Fig 13 – Comparison graph of FDR.

proposed and existing classifiers. When using our proposed method DNN_JOA the value of FDR of normal image is 17.1, bacterial blight is 19.5, blast is 10, brown spot is 26.6 and sheath rot is 25. When using ANN classifier the FDR of normal image is 32.82, bacterial blight is 33.6, blast is 30.1, brown spot is 36.5 and sheath rot is 33. When using DAE classifier the value of FDR of normal image is 27.9, bacterial blight is 29.1, blast is 25, brown spot is 31.4 and sheath rot is 34.5. When using DNN classifier the FDR of normal image is 22.67, bacterial blight is 22.6, blast is 21.2, brown spot is 29.4 and sheath rot is 27.3.

Fig. 14 represents the comparison graph of NPV for the five classes with respect to the four classifiers which includes the proposed and existing classifiers. When using our proposed method DNN_JOA the value of NPV of normal image is 91.2, bacterial blight is 95, blast is 97.4, brown spot is 93.6 and sheath rot is 96.1. When using ANN classifier the NPV of normal image is 75.6, bacterial blight is 74.89, blast is 82.56, brown spot is 71.54 and sheath rot is 77.9. When using DAE classifier the value of NPV of normal image is 79.2, bacterial blight is 87.45, blast is 90.56, brown spot is 83.78 and sheath rot is 81.54. When using DNN classifier the NPV of normal image is 88.5, bacterial blight is 91.45, blast is 94.5, brown spot is 89.78 and sheath rot is 87.

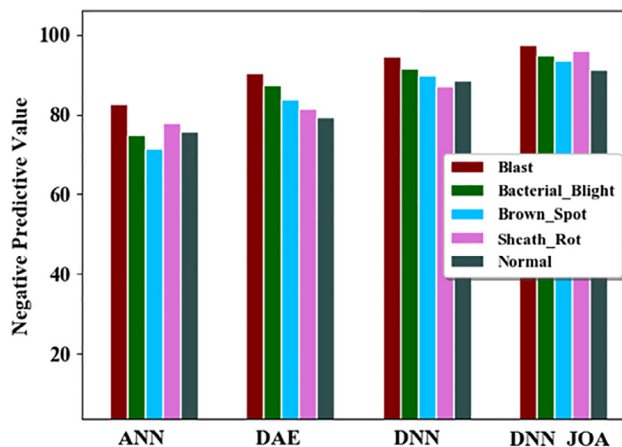


Fig 14 – Comparison graph of NPV.

Fig. 15 represents the comparison graph of precision for the five classes with respect to the four classifiers which includes the proposed and existing classifiers. When using our proposed method DNN_JOA the precision value of normal image is 73, bacterial blight is 80.4, blast is 92.8, brown spot is 85 and sheath rot is 75. When using ANN classifier the precision value of normal image is 54, bacterial blight is 65, blast is 69.56, brown spot is 58.4 and sheath rot is 57.4. When using DAE classifier the precision value of normal image is 65.32, bacterial blight is 70.4, blast is 74.2, brown spot is 65 and sheath rot is 63. When using DNN classifier the precision value of normal image is 68.9, bacterial blight is 77.56, blast is 84.9, brown spot is 73 and sheath rot is 70.2.

Fig. 16 represents the comparison graph of TPR for the five classes with respect to the four classifiers which includes the proposed and existing classifiers. When using our proposed method DNN_JOA the TPR value of normal image is 75.6, bacterial blight is 89.5, blast is 92.6, brown spot is 85.5 and sheath rot is 75.3. When using ANN classifier the TPR value of normal image is 52, bacterial blight is 69, blast is 70, brown spot is 64.5 and sheath rot is 61. When using DAE classifier the TPR value of normal image is 59.2, bacterial blight is 72.5, blast is 74, brown spot is 69.4 and sheath rot is 65. When using DNN classifier the TPR value of normal image is 65.1, bacterial blight is 79, blast is 82.6, brown spot is 72.6 and sheath rot is 68.

Fig. 17 represents the comparison graph of TNR for the five classes with respect to the four classifiers which includes the proposed and existing classifiers. When using our proposed method DNN_JOA the TNR value of normal image is 90.7, bacterial blight is 91, blast is 98.1, brown spot is 94.5 and sheath rot is 95.9. When using ANN classifier the TNR value of normal image is 73.6, bacterial blight is 87.5, blast is 82.2, brown spot is 83.6 and sheath rot is 81. When using DAE classifier the TNR value of normal image is 85.5, bacterial blight is 88.2, blast is 93.2, brown spot is 85 and sheath rot is 84. When using DNN classifier the TNR value of normal image is 85.6, bacterial blight is 89.6, blast is 94.5, brown spot is 88.4 and sheath rot is 89.

Fig. 18 represents the graph for the comparison of cross entropy loss function of our proposed method DNN_JOA with the existing methods. The loss function is compared with respect to the probability. The value of loss function decreases

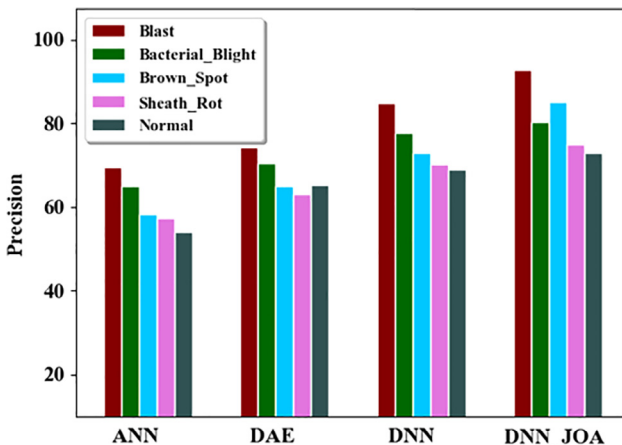


Fig 15 – Comparison graph of precision.

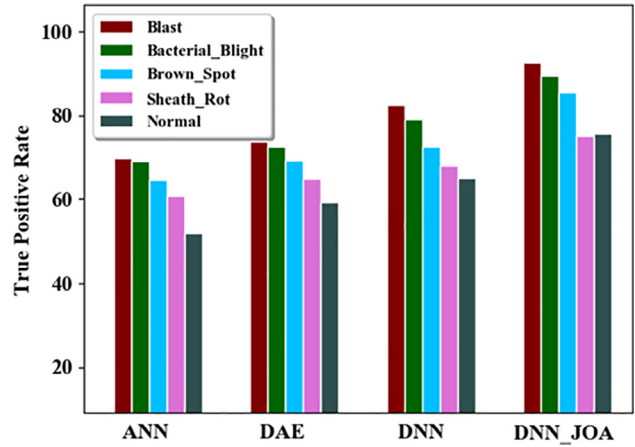


Fig 16 – Comparison graph of TPR.

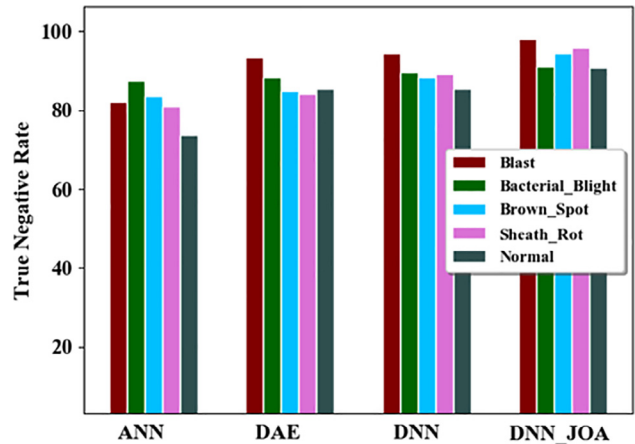


Fig 17 – Comparison graph of TNR.

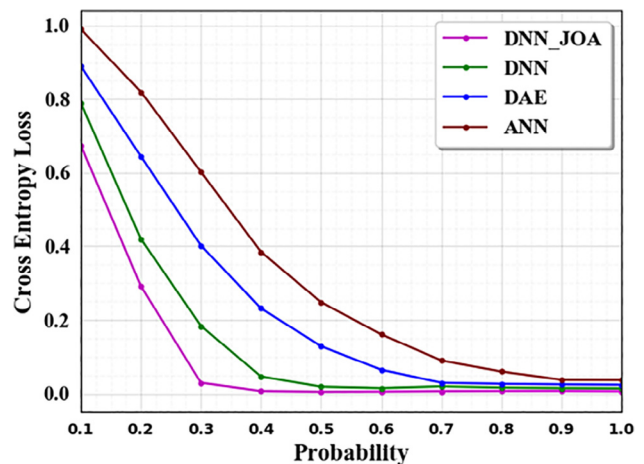


Fig 18 – Cross entropy loss comparison.

with the increase in the probability value. From Fig. 18 it is clear that our proposed DNN_JOA method attained the lowest cross entropy loss.

Fig. 19 shows the comparison graph of training and testing accuracy. For the training process number of samples consid-

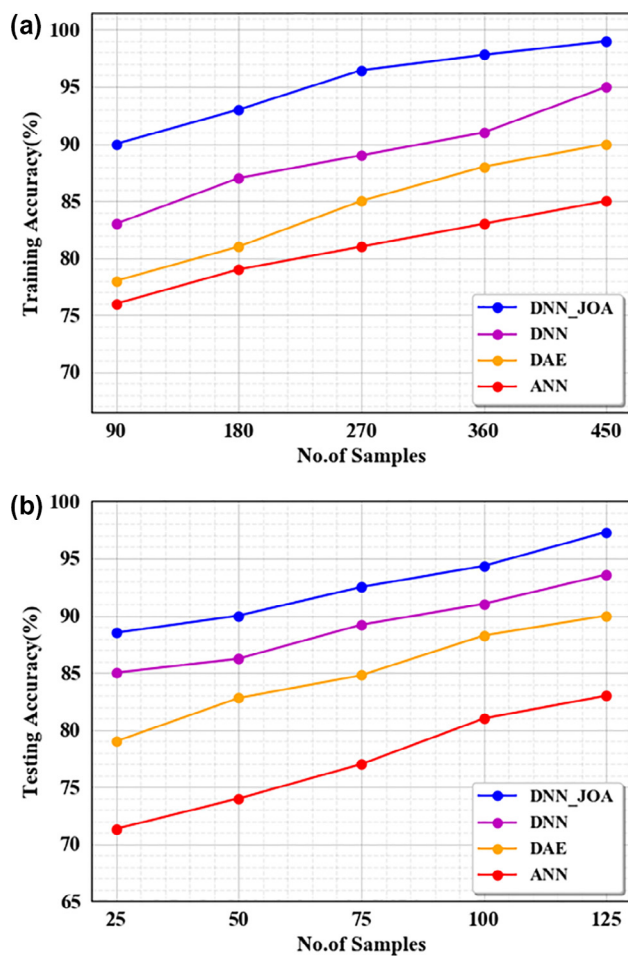


Fig 19 – (a) Training accuracy (b) Testing accuracy.

ered is 450 and for testing process 125 samples are considered. Both the training and testing accuracy increases with the increase in the number of samples considered. On comparing both the training accuracy is highly attained as 99% with 450 samples and the testing accuracy is highly attained as 97% with 125 samples by using the DNN_JOA method. The graph shows that the training accuracy is higher than the testing accuracy.

6. Conclusion

The images of paddy leaves are directly captured from the farm field for normal and the diseases like bacterial blight, brown spot, sheath rot and blast. In pre-processing, to remove the background, the RGB images are converted into HSV images and based on the hue part masking is performed. A clustering method is used for the segmentation of diseased portion and normal portion. By using the proposed DNN_JOA method, classification of diseases is carried out in which the best weights are selected by the JOA. A feedback loop is created in our system to precise the stability. The experimental results are evaluated and compared with ANN, DAE and DNN by evaluating accuracy, precision, F1-score, TNR, TPR, FPR, FNR, FDR and NPV. When compared with other classifiers

DNN_JOA method achieved high accuracy of 98.9% for the blast affected, 95.7% for the bacterial blight, 92% for the sheath rot, 94% for the brown spot and 90.57% for the normal leaf image. On comparing the training and testing accuracy, the testing accuracy attained the highest of 97% by using the DNN_JOA classifier, 83% by using the ANN classifier, 90% by using the DAE classifier and 93.5% by using the DNN classifier. In future, to improve the recognition and the classification of plant diseases, any improved method can be used to achieve the best performance by reducing the false classification.

Declaration of Competing Interest

The authors declared that there is no conflict of interest.

REFERENCES

- [1] Xuan Vo-Tong. Rice production, agricultural research, and the environment. In Vietnam's rural transformation: Routledge; 2018. p. 185–200.
- [2] Pantazi XE, Moshou D, Tamouridou AA. Automated leaf disease detection in different crop species through image features analysis and one class classifiers. *Comput Electron Agric* 2019;156:96–104.
- [3] El-kazzaz MK, Salem EA, Ghoneim KE, Elsharkawy MM, El-Kot GA, Kalboush ZA. Integrated control of rice kernel smut disease using plant extracts and salicylic acid. *Arch Phytopathol Plant Protect* 2015;48(8):664–75.
- [4] Yusof M, Mohd NF, Rosli M, Othman R, Mohamed MHA A. M-DCocoa: M-agriculture expert system for diagnosing cocoa plant diseases. *Proc. International Conference on Soft Computing and Data Mining*. 2018 2018:363–71.
- [5] Kim, Dae-Young, Kadam A, Shinde S, Saratale RG, Patra J, Ghodake G. Recent developments in nanotechnology transforming the agricultural sector: a transition replete with opportunities. *J Sci Food Agric* 2018;98(3):849–64.
- [6] Astonkar, Shweta R, Shandilya VK. Detection and Analysis of Plant Diseases Using Image Processing. *Int Res J Eng Technol* 2018;5(4):3191–3.
- [7] Singh A, Kumar B, Ganapathysubramanian SS, Singh A. Deep learning for plant stress phenotyping: trends and future perspectives. *Trends Plant Sci* 2018;23(10):883–98.
- [8] Kamal M, Mahanijah ANI, Masazhar FAR. Classification of leaf disease from image processing technique. *Indonesian J Elect Eng Comput Science* 2018;10(1):191–200.
- [9] Patrício D, Inácio RR. Computer vision and artificial intelligence in precision agriculture for grain crops: a systematic review. *Comput Electron Agric* 2018;153:69–81.
- [10] Prajapati BH, Shah JP, Dabhi VK. Detection and classification of rice plant diseases. *Intell Decis Technol* 2017;11(3):357–73.
- [11] Barbedo JG, Arnal LV, Koenigkan TTS. Identifying multiple plant diseases using digital image processing. *Biosyst Eng* 2016;147:104–16.
- [12] Sladojevic S, Arsenovic M, Anderla A, Culibrk D, Stefanovic D. Deep neural networks based recognition of plant diseases by leaf image classification. *Comput Intell Neurosci* 2016:1–11.
- [13] Mohanty P, Sharada DP, Hughes MS. Using deep learning for image-based plant disease detection. *Front Plant Sci* 2016;7(1419):1–10.
- [14] Mahlein A-K. Plant disease detection by imaging sensors—parallels and specific demands for precision agriculture and plant phenotyping. *Plant Dis* 2016;100(2):241–51.

- [15] Pinki F, Tazmim N, Khatun SMM Islam. Content based paddy leaf disease recognition and remedy prediction using support vector machine. In: In: Proc. In Computer and Information Technology (ICCIT). 20th International Conference; 2017. p. 1–5.
- [16] Lu Y, Yi S, Zeng N, Liu Y, Zhang Y. Identification of rice diseases using deep convolutional neural networks. *Neurocomputing* 2017;267:378–84.
- [17] Dhingra G, Kumar V, Joshi HD. A novel computer vision based neutrosophic approach for leaf disease identification and classification. *Measurement* 2019;135:782–94.
- [18] Nidhis AD, Pardhu CNV, Reddy KC, Deepa K. Cluster based paddy leaf disease detection, classification and diagnosis in crop health monitoring unit. *Comput Aided Interven Diagnost Clinic Med Images* 2019;31:281–91.
- [19] Islam T, Sah M, Baral S, Choudhury RR. A faster technique on rice disease detection using image processing of affected area in agro-field. In: In: Proc. Second International Conference on Inventive Communication and Computational Technologies. p. 62–6.
- [20] Devi T, Gayathri PN. Image processing based rice plant leaves diseases in Thanjavur Tamilnadu. *Cluster Comput* 2018:1–14.
- [21] Kaya A, Keceli AS, Catal C, Yalic HY, Temucin H, Tekinerdogan B. Analysis of transfer learning for deep neural network based plant classification models. *Comput Electron Agric* 2019;158:20–9.
- [22] dos Santos FA, Freitas DM, da Silva GG, Pistori H, Folhes MT. Weed detection in soybean crops using ConvNets. *Comput Electron Agricul* 2017;143:314–24.
- [23] Rao RV. Jaya: A simple and new optimization algorithm for solving constrained and unconstrained optimization problems. *International Journal of Industrial Engineering Computations* 2016;7:19–34.